Kazrin regulates keratinocyte cytoskeletal networks, intercellular junctions and differentiation

Lisa M. Sevilla[1,2], Rachida Nachat[1], Karen R. Groot[3] and Fiona M. Watt[1,2,*]

[1]Epithelial Cell Biology Laboratory, Cancer Research UK Cambridge Research Institute, Li Ka Shing Centre, Robinson Way, Cambridge CB2 0RE, UK
[2]Wellcome Trust Centre for Stem Cell Research and Department of Genetics, University of Cambridge, Tennis Court Road, Cambridge CB2 1QR, UK
[3]National Cancer Research Institute, 61 Lincoln's Inn Fields, PO Box 123, London WC2A 3PX, UK
*Author for correspondence (e-mail: fiona.watt@cancer.org.uk)

Accepted 4 August 2008
Journal of Cell Science 121, 3561-3569 Published by The Company of Biologists 2008
doi:10.1242/jcs.029538

Summary

Kazrin is an evolutionarily conserved protein that is upregulated during keratinocyte terminal differentiation. Kazrin localizes to desmosomes and binds the epidermal cornified envelope protein periplakin. Kazrin overexpression in human epidermal keratinocytes caused profound changes in cell shape, reduced filamentous actin, reorganized keratin filaments, and impaired assembly of intercellular junctions. These effects were attributable to decreased Rho activity in kazrin-overexpressing cells. Kazrin overexpression also stimulated terminal differentiation and reduced clonal growth in culture. Knockdown of kazrin decreased expression of differentiation markers and stimulated proliferation without changing total Rho activity. We conclude that kazrin is a dual regulator of intercellular adhesion and differentiation in keratinocytes and regulates these processes by Rho-dependent and -independent mechanisms.

Supplementary material available online at
http://jcs.biologists.org/cgi/content/full/121/21/3561/DC1

Key words: Rho GTPases, Cytoskeleton, Desmosomes, Keratinocyte, Terminal differentiation

Introduction

The outermost layers of the epidermis, the stratum corneum, form a protective barrier between the body and the external environment. Cells in the stratum corneum assemble a structure known as the cornified envelope at the inner surface of the plasma membrane (Candi et al., 2005). The cornified envelope consists of a meshwork of insoluble, transglutaminase cross-linked proteins and lipids essential for the mechanical integrity and water impermeability of the skin. As stratum corneum cells detach from the epidermal surface they are replaced by proliferation of undifferentiated basal layer cells, whose progeny terminally differentiate as they move through the suprabasal layers. The balance between proliferation and differentiation in the epidermis is influenced by signals emanating from the basement membrane, intercellular junctions and their associated cytoskeletal networks (Watt, 2001; Wheelock and Johnson, 2003; Yin and Green, 2004).

One of the proteins incorporated into the cornified envelope is periplakin (Ruhrberg et al., 1997), a member of the plakin family of proteins that link cytoskeletal networks to each other and to membrane-associated adhesive sites (Jefferson et al., 2004). The periplakin C terminus directly binds intermediate filaments, while the N terminus associates with cortical actin and desmosomes (DiColandrea et al., 2000). We recently reported that the N terminus of periplakin binds a novel, highly conserved protein, kazrin (Groot et al., 2004). Thus far, four transcript variants of kazrin have been identified encoding three proteins with different N termini (kazrinA, B and C). Kazrin localizes to the nucleus, cell membrane, desmosomes and adherens junctions (Gallicano et al., 2005; Groot et al., 2004).

The direct binding of intermediate filaments by periplakin, together with the subcellular distributions of periplakin and kazrin, suggest that both proteins participate in the known interplay between desmosomes and adherens junctions (Huen et al., 2002; Lewis et al., 1997; Vasioukhin et al., 2001). Kazrin is widely expressed, suggestive of a function that extends beyond assembly of the cornified envelope (Groot et al., 2004). In the present article, we have uncovered new roles for kazrin in regulating cytoskeletal organization, intercellular junction assembly and differentiation.

Results

Expression of kazrin increases during Ca^{2+}-induced stratification

Our previous data showed that kazrin localizes to desmosomes, the interdesmosomal plasma membrane and the nucleus of epidermal keratinocytes both in vitro and in vivo (Groot et al., 2004). However, the expression and subcellular localization of kazrin during the early stages of intercellular junction assembly and terminal differentiation have not been investigated. To examine this, keratinocytes were cultured to confluence in low Ca^{2+} medium (containing 0.09 mM Ca^{2+}), and then transferred to standard ('high Ca^{2+}') medium containing 1.8 mM Ca^{2+} to stimulate intercellular junction assembly and accumulation of terminally differentiated cells (Green et al., 1987; Vasioukhin et al., 2000; Watt et al., 1984).

We found that endogenous kazrin protein levels increased twofold following 24 hours incubation in high Ca^{2+} medium (Fig. 1A). Levels were also elevated at 48 hours. However, there was a decrease at 72 hours, which probably reflects kazrin becoming insoluble as it is incorporated into the cornified envelope (Groot et al., 2004). Within 6 hours of addition of Ca^{2+}, kazrin had accumulated at cell-cell borders where it colocalized with the desmosomal marker, desmoplakin (Fig. 1B,C). By 24 hours, kazrin and desmoplakin levels at cell-cell borders were further increased

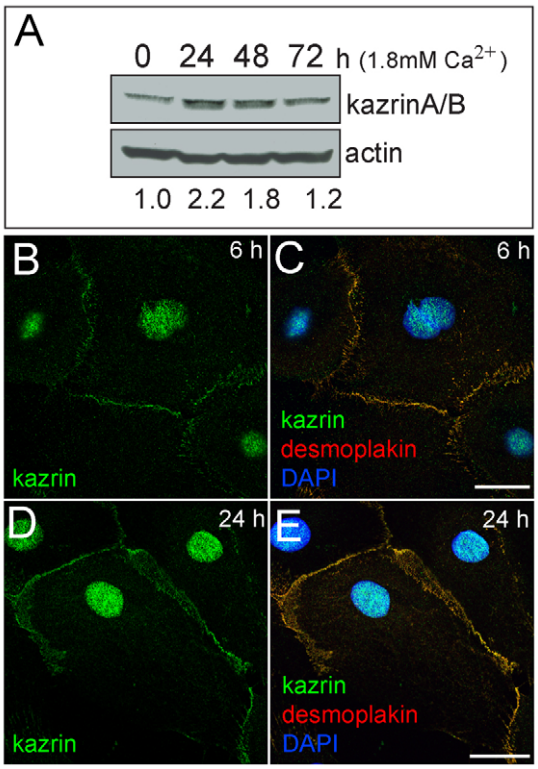

Fig. 1. Kazrin protein levels increase during Ca^{2+}-induced accumulation of terminally differentiating cells. (A) Immunoblotting of lysates from keratinocytes plated in the absence of feeders in low Ca^{2+} medium and then incubated in high Ca^{2+} medium for 0, 24, 48 or 72 hours. Band intensities were quantified and kazrin levels relative to t=0 normalized to actin are indicated below immunoblots. (B-E) Immunostaining for kazrin (green) and desmoplakin (red) in keratinocytes that were incubated in high Ca^{2+} medium for 6 (B,C) or 24 (D,E) hours. Nuclei were detected with DAPI counterstain (blue). Bars, 25 μm.

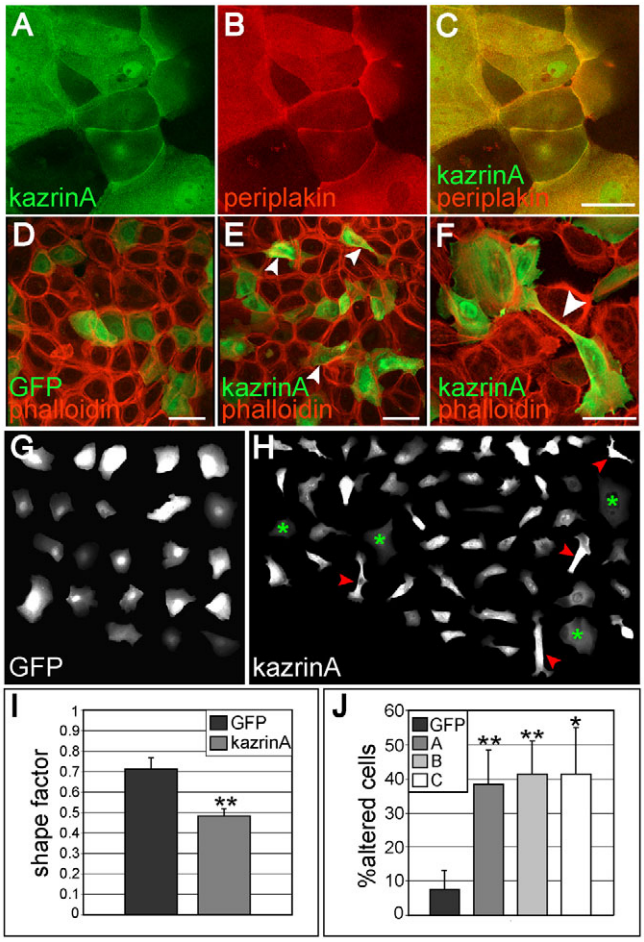

Fig. 2. Kazrin overexpression alters keratinocyte shape. (A-C) Primary human keratinocytes infected with HA-kazrinA retroviral vector (green). Note that HA-kazrinA colocalizes with periplakin (red) at cell-cell borders (C). (D-F) Primary human keratinocytes transiently expressing HA-kazrinA (E,F; green) have shape abnormalities and extend membrane projections (arrowheads) over neighbouring cells in contrast to control cells expressing GFP (D; green). F-actin is detected with phalloidin (red). Images are composites of z-stacks. Bars, 40 μm. (G-I) Shape factor analysis of keratinocytes transiently expressing GFP (G) or HA-kazrinA (H). In (H) examples of cells with high levels of kazrin are marked with an arrowhead, and cells with low levels are marked with an asterisk. The Discovery-1 biorobot was used to collect four images per coverslip on microscope slides containing three coverslips of transfected keratinocytes per condition. Transfectants were identified by GFP fluorescence or staining with HA-specific antibody. Using Metamorph 7 software, transfected cells were traced, copied and pasted into a new file. At least 20 transfectants were traced per condition, per experiment. Following thresholding, the shape factor was calculated. (G,H) Examples of traced keratinocytes from one experiment. (I) Summary of shape factor analysis; data are the means ± s.d. from four independent experiments. Statistical significance relative to GFP control was assessed with the paired Student's t-test (**P<0.005, n=4). (J) Keratinocytes transiently expressing GFP, HA-kazrinA, B or C were scored as 'altered' if they exhibited loss of the normal round or cuboidal shape characteristic of an undifferentiated keratinocyte and/or loss of cortical actin. The total numbers of cells counted were: GFP, 1060; kazrinA, 1084; kazrinB, 621; kazrinC, 636. Data are the means ± s.d. of five (kazrinB and C) or eight (GFP and kazrinA) independent experiments. Statistical significance relative to GFP control was assessed with the unpaired Student's t-test (**P≤0.0005, *P≤0.005; n≥5).

(Fig. 1D,E). At all time points kazrin was also detected in the nucleus (Fig. 1B-E). We conclude that although kazrin is expressed in all the living layers of the epidermis (Groot et al., 2004), it is upregulated in suprabasal, differentiating cells.

Overexpression of kazrin isoforms causes cell shape changes and impaired remodelling of cytoskeletal networks in response to Ca^{2+}

As we observed an increase in kazrin expression during keratinocyte differentiation, we evaluated the consequences of overexpressing kazrin in undifferentiated primary human keratinocytes. When expressed at moderate levels in all cells through retroviral infection, N-terminally HA-tagged kazrinA was present in the nucleus and colocalized with periplakin at cell-cell borders and the interdesmosomal plasma membrane (Fig. 2A-C). Thus the distribution of overexpressed kazrinA was the same as that of the endogenous protein (Fig. 1B-E) (Groot et al., 2004).

The consequences of higher levels of kazrinA overexpression were evaluated by transient transfection of human keratinocytes. Cells were transfected and incubated overnight in low Ca^{2+} medium, and then transferred to high Ca^{2+} medium for 2 hours in order to stimulate assembly of adherens junctions and desmosomes (Green et al., 1987; Vasioukhin et al., 2000; Watt et al., 1984). Cells transiently overexpressing N-terminally HA-tagged kazrinA exhibited profound changes in cell shape compared to cells transfected with a control GFP construct (Fig. 2D-F). KazrinA overexpression resulted in loss of the normal cuboidal shape characteristic of epithelial cells, and this was reflected in a

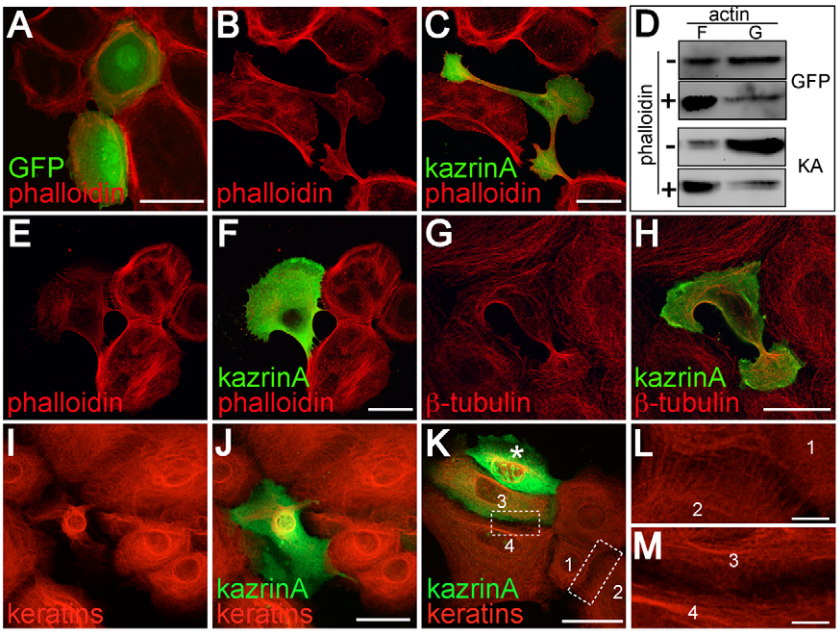

Fig. 3. KazrinA overexpression affects cytoskeletal organization. (A-C,E-M) Single confocal slice images of keratinocytes transiently transfected with GFP (A; green) or HA-kazrinA (B,C,E-M; green). F-actin was detected with phalloidin (A-C,E,F; red), microtubules with a β-tubulin-specific antibody (G,H; red), and intermediate filaments with a pan keratin-specific antibody (I-M; red). (D) Immunoblot showing the proportion of F-actin (pellet; F) versus G-actin (supernatant; G) following centrifugation of lysates of cells transduced with GFP (upper panels) or kazrinA (KA; lower panels). Phalloidin was added to cell lysates as a positive control for detection of F-actin. L and M are enlargements of borders between cells 1 and 2, and cells 3 and 4, respectively (boxed with broken lines), in K. Asterisk in K marks cell with collapsed intermediate filament cytoskeleton. Bars, 40 μm (A-K), 3 μm (L,M).

statistically significant decrease in shape factor [defined as $4\pi\times$ (area/perimeter^2); Fig. 2G-I]. Although the average cell area available for contact with the substrate was not significantly affected, the average perimeter of kazrinA-overexpressing cells was dramatically increased, reflecting the kazrinA-induced shape changes (data not shown). Keratinocytes expressing higher levels of kazrinA (Fig. 2H, arrowheads) exhibited more dramatic changes in shape than cells with lower expression levels (Fig. 2H, asterisks). KazrinA-overexpressing cells extended membrane projections over neighbouring cells (Fig. 2E,F, arrowheads), often appearing to be in the process of stratifying. Overexpression of kazrinA, B and C isoforms resulted in similar changes in keratinocyte shape (Fig. 2J). We therefore focused on the most evolutionarily conserved isoform, kazrinA, in subsequent experiments.

Compared with control cells transfected with GFP (Fig. 3A), cells overexpressing kazrinA exhibited abnormal spreading and stretching (Fig. 3B,C,E-H). KazrinA overexpression impaired formation of the cortical actin band normally present in keratinocytes (see Fig. 3A) and led to an overall decrease in filamentous actin (F-actin), detected by phalloidin (Fig. 3B,C,E,F). This was confirmed by determining the ratio of F- to G-actin in lysates of keratinocytes transduced with GFP or kazrinA retroviral vectors (Fig. 3D). The F-actin:G-actin ratio in cells overexpressing kazrinA was 0.12, compared with 0.3 in cells overexpressing GFP (Fig. 3D). Lysates were incubated with phalloidin as a positive control for accumulation of F-actin.

In contrast to the effects of kazrinA overexpression on the actin cytoskeleton, the microtubule network was intact in kazrinA

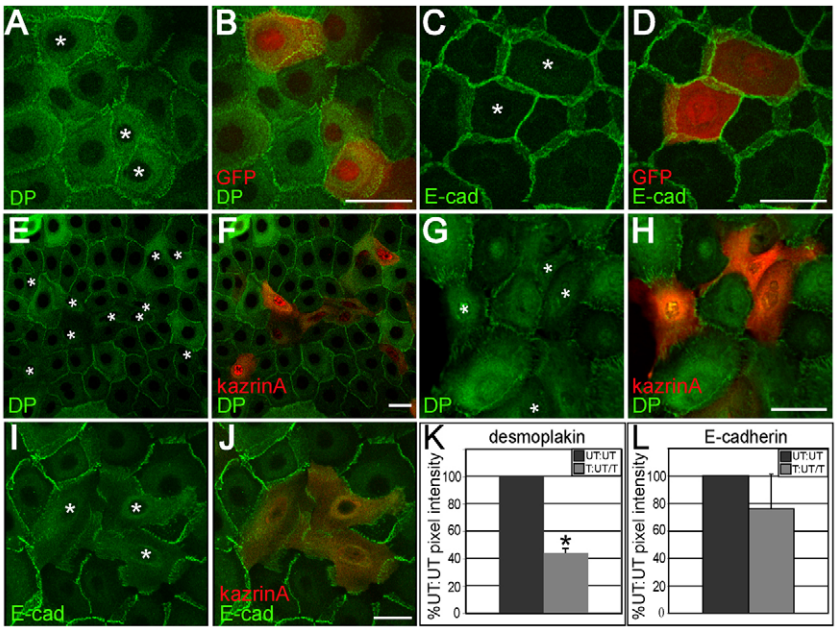

Fig. 4. KazrinA overexpression impairs intercellular junction assembly. (A-J) Keratinocytes were transiently transfected with GFP (A-D) or HA-kazrinA (E-J), in medium containing 0.09 mM Ca^{2+}. Twenty-four hours post-transfection, cells were incubated in medium containing 1.8 mM Ca^{2+} for 2 hours, then fixed and directly visualized for GFP (B,D; red) or labelled with antibodies specific for HA (F,H,J; red), desmoplakin (A,B,E-H; green) or E-cadherin (C,D,I,J; green). Asterisks indicate transfected cells. (A-H) single confocal slices; (I,J) composites of *z*-stacks. Bars, 40 μm. (K,L) Quantification of average pixel intensity of desmoplakin (K) and E-cadherin (L) immunostaining at cell-cell borders. Border between a kazrin-transfected cell and an untransfected or a kazrin-transfected cell is designated T:UT/T. Border between untransfected cells is designated UT:UT. Values are expressed relative to UT:UT. Data are the means ± s.d. of three independent experiments. Statistical significance was determined with paired Student's *t*-test (*P<0.05; n=3).

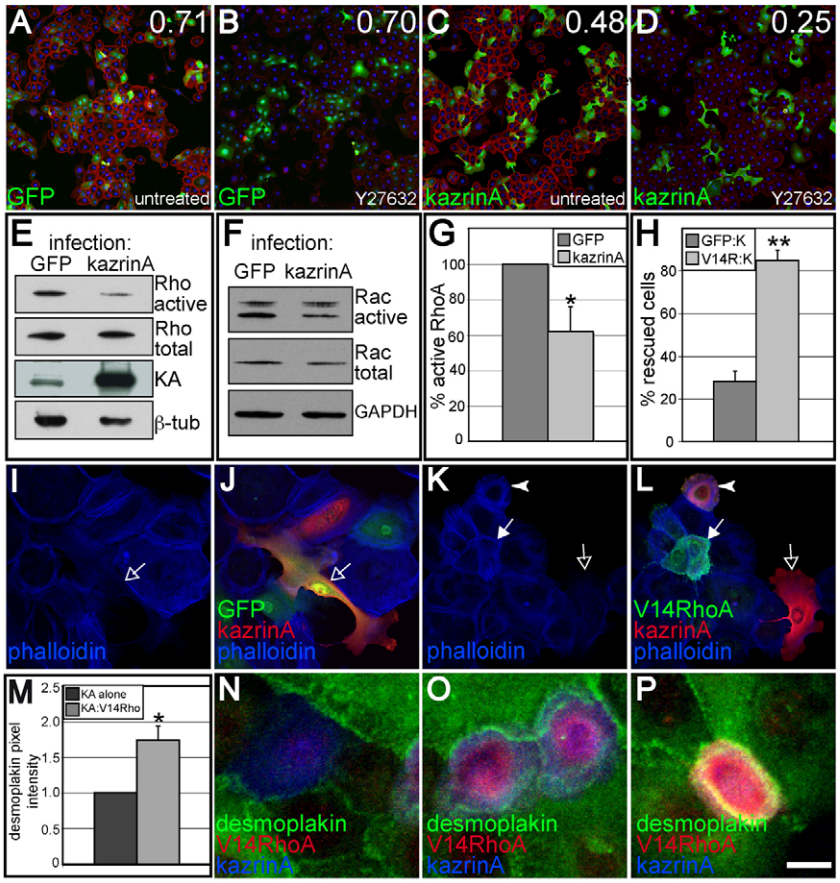

Fig. 5. KazrinA reduces Rho activity. (A-D) Single confocal slices of keratinocytes transiently transfected with GFP (green; A,B) or HA-kazrinA (green; C,D) in the absence (A,C) or presence (B,D) of Y27632. F-actin was visualized with phalloidin (red) and nuclei with DAPI (blue). Bar, 200 μm. Numbers correspond to shape factors. (E-G) Rho activity is reduced in keratinocytes infected with HA-kazrinA whereas Rac activity is unaffected. (E,F) Pulldown assays using GST-Rhotekin Rho-binding domain (E) or GST-PAK p21 binding domain (F) coupled to glutathione agarose in keratinocyte lysates infected with GFP or HA-kazrinA (active). 5% of each lysate used for the pulldown assays was probed with antibodies to Rho or Rac1 (total), kazrinA (KA), β-tubulin or (β-tub) GAPDH. (G) Quantification of three independent Rho pulldown experiments from different infections. Percentage active Rho was calculated by dividing the band intensity of Rho active with the band intensity of Rho total. Values are expressed relative to percentage of active Rho in GFP-infected cells as 100%. Data are the mean ± s.d. Statistical significance was calculated using the paired Student's *t*-test (**P*<0.05, *n*=3). (H-L) Rescue of kazrinA-induced changes in shape and actin cytoskeleton by dominant active V14RhoA. (H) Keratinocytes co-expressing kazrinA with GFP or V14RhoA were scored as 'rescued' if they had normal morphology and a cortical actin band. At least 100 cells were counted per transfection in each experiment. Data are the means ± s.d. of three experiments. Statistical significance relative to GFP control was assessed by the paired Student's *t*-test (***P*≤0.0005; *n*=3). (I-L) Composite images of *z*-stacks showing keratinocytes co-transfected with HA-kazrinA (red) and either GFP (green; I,J) or myc-tagged V14RhoA (green; K,L). F-actin was visualized with phalloidin (blue). Open arrows indicate cells expressing kazrinA alone or together with GFP. Filled arrow indicates cell solely expressing V14RhoA and arrowhead indicates cell expressing both kazrinA and V14RhoA. Bars, 60 μm. (M-P) Desmoplakin levels are increased at cell-cell borders of kazrinA and V14RhoA co-transfectants, relative to cells expressing kazrinA alone. (M) Quantification of average pixel intensity of desmoplakin at cell-cell borders of cells expressing kazrinA alone or in combination with V14RhoA. Data are the means ± s.d. of three independent experiments. Statistical significance was determined with paired Student's *t*-test (**P*<0.05; *n*=3). (N-P) Desmoplakin (green) levels at borders of cell solely expressing kazrinA (blue; N) are lower than those in cells co-expressing V14RhoA (red; O,P). Images are composites of *z*-stacks. Bar, 7.5 μm.

transfectants (Fig. 3G,H). However, keratin filaments were reorganized and did not extend into cell-cell contacts (Fig. 3I-M). Similar effects on cell shape and the cytoskeleton were observed in cells transfected with C-terminally HA-tagged or N- or C-terminally FLAG-tagged kazrinA, B or C constructs (data not shown).

Overexpression of kazrinA inhibits desmosome assembly

We next investigated whether kazrinA overexpression affected intercellular junction assembly. As before, keratinocytes were transiently transfected in low Ca^{2+} medium and then transferred to standard medium for 2 hours prior to analysis. Overexpression of GFP did not prevent the accumulation of desmoplakin at desmosomes or E-cadherin at adherens junctions (Fig. 4A-D). By contrast, cells overexpressing kazrinA exhibited a dramatic reduction in desmoplakin staining at cell-cell borders (Fig. 4E-H,K). Although kazrinA transfection did not prevent E-cadherin localization to cell-cell borders, E-cadherin organisation did appear to be altered relative to cells transfected with GFP (Fig. 4I,J,L).

KazrinA overexpression decreases Rho GTPase activity

We examined whether modulation of cell signalling pathways known to regulate the cytoskeleton and cell-cell adhesion would affect kazrinA-induced cell shape changes. Keratinocytes were incubated following transfection and during the 2 hour Ca^{2+} switch in the presence or absence of small molecule inhibitors of Rho kinase (ROCK; Fig. 5A-D), PI 3-kinase and the EGF receptor (data not shown). Cell shape, as quantified by calculating the shape factor, of GFP transfectants was not significantly affected by the inhibitor treatments (Fig. 5A,B and data not shown). Treatment with inhibitors of PI 3-kinase and the EGF receptor did not result in statistically significant changes in the shape factor of kazrinA transfectants (data not shown). By contrast, treatment with the ROCK inhibitor Y27632 resulted in a dramatic exacerbation of the kazrinA-induced cell shape changes, the shape factor decreasing from 0.48 in untreated kazrinA transfectants to 0.25 in treated cells (Fig. 5C,D).

ROCK is activated by GTP-bound RhoA and RhoC and promotes the formation of contractile actin stress fibres (Riento and Ridley, 2003). The observations of decreased F-actin, reorganized intermediate filaments, defects in intercellular junction assembly and hypersensitivity to ROCK inhibition upon kazrinA overexpression suggested a reduction in Rho activity (Braga et al., 1997; Jaffe and Hall, 2005; Waschke et al., 2006). To directly assess levels of active Rho, we stably transduced keratinocytes with retroviral vectors expressing GFP or kazrinA and performed pull-downs of cell lysates with the Rho binding domain of Rhotekin fused to GST (Fig. 5E,G). KazrinA overexpression resulted in an average decrease of 40% in levels of active Rho relative to the GFP control (Fig. 5E,G). By contrast, there was no

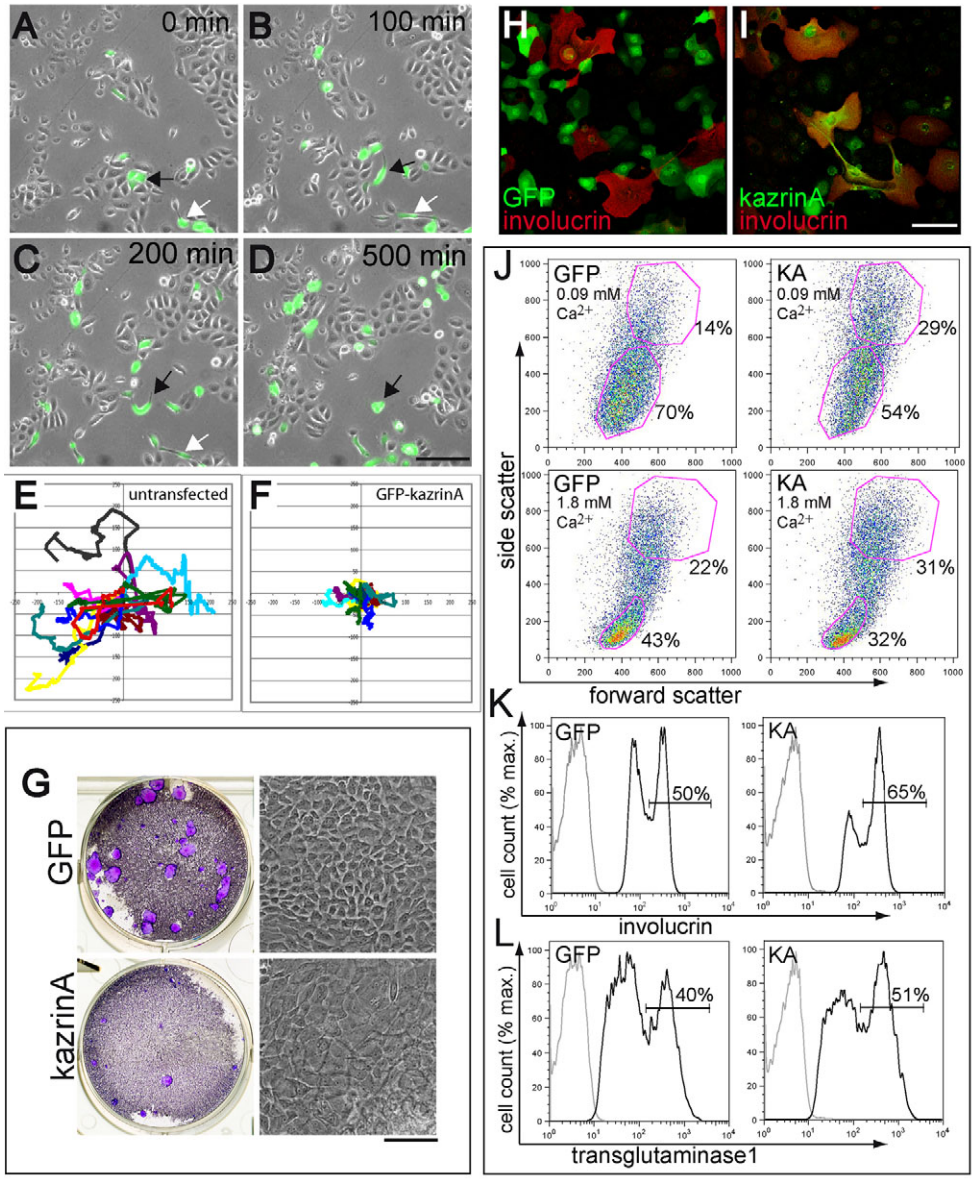

Fig. 6. Kazrin induces terminal differentiation. (A-D) Still frames from a time-lapse recording (see Movie 1 in supplementary material) of keratinocytes transiently expressing GFP-kazrinA (green). The times in each frame are minutes of recording. Black and white arrows follow the paths of two transfected cells. (E,F) Vector diagrams tracking migration of (E) ten untransfected and (F) ten GFP-kazrinA-expressing cells in Movie 1 in supplementary material. (G) Clonogenicity assay in which 10^3 keratinocytes transduced with either GFP or HA-kazrinA were plated onto mitomycin-C-treated J2 feeders. Two weeks post-plating, cells were fixed and stained with Rhodamine B (left panels) or examined by phase-contrast microscopy (right panels). (H,I) Single confocal slice images of keratinocytes expressing GFP (H; green) or HA-kazrinA (I; green), labelled with antibodies specific for involucrin (red) 48 hours post transfection. Bars, 200 μm (A-D,G), 100 μm (H,I). (J-L) Flow cytometric analysis of keratinocytes transduced with GFP or HA-kazrinA (KA), plated in the absence of feeders, and incubated for 4 days in low Ca^{2+} (J, upper panels) or standard medium (J, lower panels; K,L). Cells were gated on GFP- or HA-positive populations and then analyzed for forward and side scatter (J), or expression (dark lines) of involucrin (K) or transglutaminase 1 (L). Grey lines show control staining with secondary antibody alone (K,L). Percentages of cells in gated regions are indicated.

detectable effect of kazrinA overexpression on levels of active GTP-bound Rac1 (Fig. 5F), or on activation (as judged by tyrosine phosphorylation and membrane recruitment) of p190Rho GAP, which occurs downstream of Rac1 activation (data not shown) (Nimnual et al., 2003).

To test whether increased Rho activity could block kazrinA-induced changes in cell shape, actin organisation and desmosome assembly, keratinocytes were co-transfected with kazrinA and either GFP or dominant-active V14RhoA (Fig. 5H-P). Keratinocytes expressing kazrinA alone or together with GFP displayed the expected shape alterations and decreased cortical actin (Fig. 5I-L, open arrows). Keratinocytes expressing V14RhoA alone displayed an increase in cortical actin and stress fibres (Fig. 5K,L, filled arrows). Over 80% of cells expressing both kazrinA and V14RhoA retained the cortical actin band and cuboidal shape characteristic of untransfected keratinocytes (Fig. 5H,K,L, arrowheads). In addition, relative to cells overexpressing kazrinA alone, those co-expressing V14RhoA displayed increased desmoplakin at cell-cell borders (Fig. 5M-P). We conclude that overexpression of kazrinA results in a decrease in levels of active Rho and that this is responsible for the changes in cell shape, cytoskeletal organization and desmosome assembly.

KazrinA induces keratinocyte terminal differentiation

The morphology of kazrinA-overexpressing keratinocytes was reminiscent of either highly motile cells or cells undergoing terminal differentiation (Magee et al., 1987; Watt and Green, 1982). To examine the effects of kazrin on cell motility, we performed video microscopy on keratinocytes transiently transfected with GFP-kazrinA. GFP-kazrinA transfectants did not display increased motility. The cells stretched and elongated but did not migrate far from their initial positions (Fig. 6A-F, green cells, black and white arrows; see Movie 1 in supplementary material). The GFP-kazrinA-expressing keratinocytes did not exhibit increased apoptosis, as assessed by TUNEL and annexin V staining (data not shown).

To determine whether the kazrinA-induced changes in cell shape reflected induction of terminal differentiation, transiently transfected cells were examined for expression of the cornified envelope protein

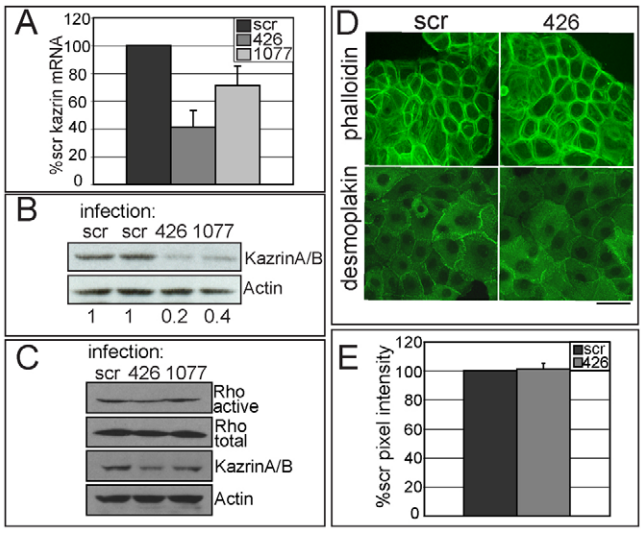

Fig. 7. Assessment of Rho activity and intercellular junctions in keratinocytes with kazrin knockdown. (A) Relative levels of kazrin mRNA as determined by quantitative PCR in keratinocytes infected with kazrin siRNA constructs 426 or 1077 or the scrambled (scr) control. Bar chart shows the average values from three independent infections (means ± s.d.). (B) Immunoblotting of protein extracts from keratinocytes expressing kazrin siRNA426, siRNA1077 or the scrambled control. Band intensities were quantified and kazrin levels, relative to the scrambled controls and normalized to actin, are indicated below immunoblots. (C) Pulldown using GST-Rhotekin Rho-binding domain coupled to glutathione agarose and lysates from keratinocytes stably expressing siRNA426, siRNA1077 or the scrambled control. 5% of each lysate used for the pulldown assays was probed with antibodies to Rho (Rho total), kazrin or actin. (D) Keratinocytes expressing siRNA426 or the scrambled control were transferred to high Ca^{2+} medium for 2 hours prior to fixation and staining for F-actin (phalloidin) or desmoplakin. Bar, 50 μm. (E) Quantification of average pixel intensity of desmoplakin immunostaining at cell-cell borders of keratinocytes expressing siRNA426 or the scrambled control. Data are the means ± s.d. of three independent experiments.

involucrin (Fig. 6H,I). At 48 hours post transfection, an increased proportion of kazrinA-overexpressing cells stained positive for involucrin (Fig. 6I) relative to those expressing GFP (Fig. 6H). Similar results were obtained with the terminal differentiation marker transglutaminase 1 (data not shown). The morphological changes induced by kazrinA, including stretching and extension of processes over neighbouring cells, were strikingly similar to the morphology of keratinocytes undergoing spontaneous terminal differentiation (Fig. 6H,I).

For further analysis of the effects of kazrin on terminal differentiation, we examined keratinocytes stably transduced with the kazrinA retroviral vector. In clonogenicity assays, kazrinA-infected cells produced substantially fewer colonies than cells transduced with GFP, with a substantial reduction in colony-forming efficiency observed in three independent experiments (Fig. 6G and data not shown). Moreover, kazrinA-infected colonies were smaller than GFP control colonies, reflecting decreased proliferative potential. KazrinA-infected cells within the colonies were enlarged, which is indicative of terminal differentiation (Fig. 6G).

Keratinocytes undergoing terminal differentiation exhibit increased forward and side scatter, measured by flow cytometry, reflecting their increase in size and granularity, respectively (Jones and Watt, 1993). Irrespective of whether the cells were grown to confluence in the absence of feeders in low Ca^{2+} (Fig. 6J, upper panels) or standard (Fig. 6J, lower panels) medium, kazrinA-infected cells showed an increase in the population with high forward and side scatter relative to GFP control cells. Consistent with the increase in forward and side scatter, kazrinA-infected cultures had a higher proportion of cells expressing the terminal differentiation markers involucrin and transglutaminase 1 than cells infected with GFP (Fig. 6K,L). Thus overexpression of kazrinA stimulates terminal differentiation, as evaluated by four different criteria (reduced clonal growth, increased forward and side scatter, and induction of involucrin and transglutaminase 1 expression).

Decreased kazrin expression results in increased proliferation and reduced terminal differentiation without affecting Rho activity

To examine the effects of decreased kazrin expression, two different siRNA (siRNA426 and 1077) sequences specific for kazrin were stably expressed in primary human keratinocytes via retroviral infection. siRNA426 reduced kazrin mRNA levels by an average of 60% relative to the scrambled siRNA control (Fig. 7A). siRNA1077 was less effective, causing an average decrease in kazrin mRNA expression of approximately 30% (Fig. 7A). Keratinocytes expressing either siRNA construct had decreased kazrin protein levels, with siRNA426 being more effective than siRNA1077 (Fig. 7B). Although kazrinA overexpression reduced levels of GTP-bound RhoA (Fig. 5E,G), we did not detect significant changes in Rho activity in keratinocytes expressing either siRNA construct relative to the control (Fig. 7C). Consistent with this, kazrin knockdown did not affect the levels of desmoplakin at cell-cell borders when monitored at 15 minute intervals for 2 hours following a Ca^{2+} switch (Fig. 7D,E and data not shown).

Although kazrin knockdown did not affect levels of active Rho, keratinocytes expressing either siRNA construct exhibited a dramatic increase in proliferation relative to control cells (Fig. 8A). We also observed a reproducible and statistically significant increase in the proportion of keratinocytes with low forward and side scatter (undifferentiated) in populations expressing siRNA426 relative to cells expressing the scrambled siRNA control (paired Student's *t*-test, $P<0.02$, $n=5$; Fig. 8B and data not shown). This correlated with statistically significant decreases in the proportions of cells expressing involucrin (paired Student's *t*-test, $P<0.02$, $n=5$; Fig. 8C and data not shown) and transglutaminase 1 (paired Student's *t*-test, $P<0.05$, $n=5$) (Fig. 8D and data not shown). siRNA1077, which was less effective at reducing kazrin levels (Fig. 7A,B) did not cause significant changes in forward and side scatter or transglutaminase 1 expression but did lead to a significant reduction in involucrin-positive cells (paired Student's *t*-test, $P<0.05$, $n=5$; data not shown). The effects of siRNA426 on keratinocyte differentiation were specific as they were rescued by co-expression of a mutated construct of kazrinA (KA-mut) which is resistant to the siRNA (Fig. 8E,F). Taken together with the overexpression data, these results indicate that kazrin plays an important role in regulating keratinocyte terminal differentiation.

Discussion

We have found that overexpression of kazrin isoforms A, B or C by transient transfection resulted in striking changes in cell morphology and cytoskeletal organization in primary human epidermal keratinocytes and led to reduced accumulation of desmoplakin and altered organization of E-cadherin at cell-cell borders. The level of GTP-bound active Rho, but not Rac1, was reduced in keratinocytes overexpressing kazrinA and the effects of

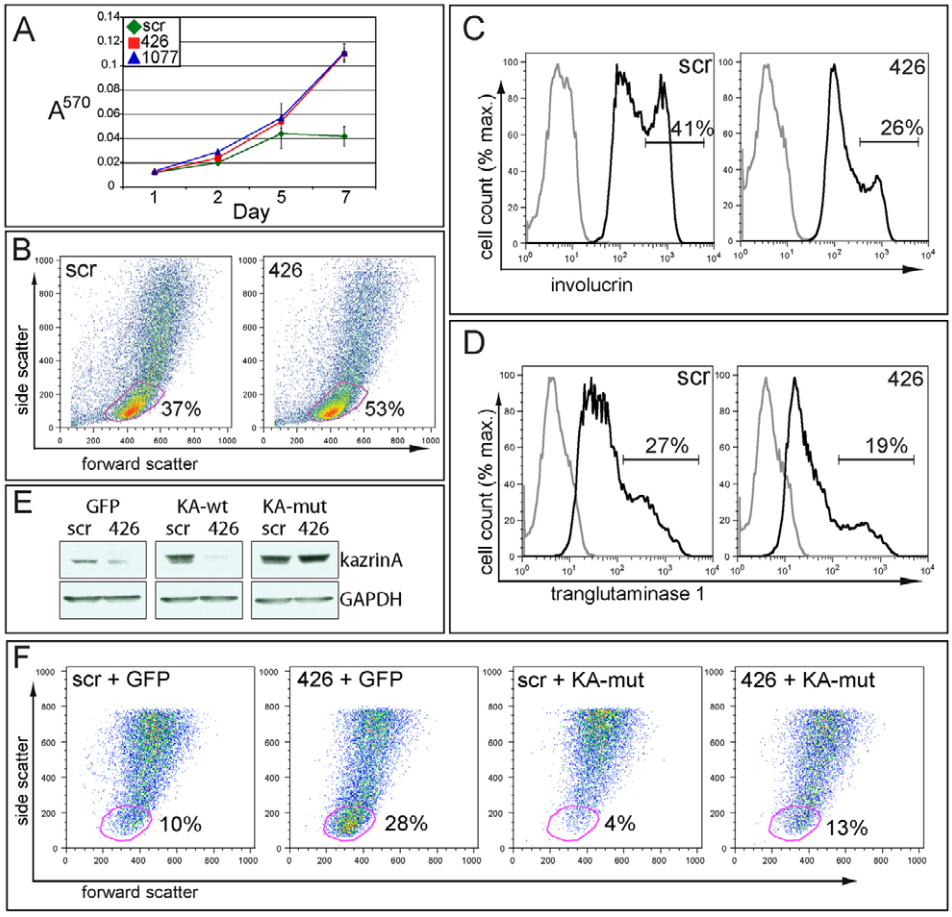

Fig. 8. Kazrin knockdown promotes proliferation and impairs terminal differentiation. (A) MTT proliferation assay with keratinocytes stably expressing kazrin siRNAs 426 or 1077 or the scrambled control. Data are the means ± s.d. (B-D) Flow cytometry analysis of keratinocytes stably expressing the scrambled control or kazrin siRNA426. Keratinocytes were plated in the absence of a feeder layer and incubated in high Ca^{2+} medium 4 days prior to harvesting. (B) Forward and side scatter; (C,D) labelling with antibodies to involucrin (C) or transglutaminase 1 (D). (E-F) Validation of siRNA specificity with a mutated kazrinA construct (KA-mut) that is resistant to siRNA426. (E) Keratinocytes were infected with siRNA426 or the scrambled control, and then either GFP, wild-type kazrinA (KA-wt) or KA-mut. Protein extracts were subjected to immunoblotting for kazrin or for GAPDH as a loading control. (F) The siRNA426-resistant kazrinA construct (KA-mut) rescues the decrease in differentiation in siRNA426-expressing keratinocytes plated in the absence of a feeder layer and incubated in high Ca^{2+} medium 4 days prior to analysis. The percentage of keratinocytes with low forward and side scatter is indicated.

kazrinA on cell shape, cytoskeletal organization and desmosome assembly were rescued by co-expression of dominant active V14RhoA. Our results are consistent with the known role of RhoA in regulating the organization of both the actin (for a review, see Jaffe and Hall, 2005) and the intermediate filament cytoskeleton (Waschke et al., 2006).

The levels of Rho GTPase activity are tightly controlled during establishment of cell-cell adhesions (Yamada and Nelson, 2007), and dysregulation can interfere with the assembly or the maintenance of intercellular junctions (Braga et al., 1997; Takaishi et al., 1997; Zhong et al., 1997). Although the mechanism by which kazrin reduces the levels of GTP-bound Rho remains to be determined, one possibility is that kazrin recruits a GTPase-activating protein to the membrane, which would stimulate GTP hydrolysis and result in inactivation of Rho. The inhibitory effect of kazrin on desmosome assembly is in good agreement with a recent study which found that dissociation of desmosomes by pemphigus vulgaris and foliaceus autoantibodies is mediated by a decrease in GTP-bound RhoA (Waschke et al., 2006).

The effects of kazrin overexpression on desmosome assembly parallel those observed when desmoglein 1 is overexpressed in transformed human keratinocytes (Hanakawa et al., 2002; Norvell and Green, 1998). Thus low levels of desmoglein 1 or kazrin can incorporate into junctions, whereas high levels disrupt cell-cell adhesion (Hanakawa et al., 2002; Norvell and Green, 1998). It is possible that upregulation of kazrin and desmoglein 1 as cells differentiate results in remodelling of basal layer desmosomes, facilitating cell movement from the basal to the suprabasal layers.

The changes in cell shape induced by kazrin are highly reminiscent of those that occur when keratinocytes leave the basal layer at the onset of terminal differentiation (Magee et al., 1987; Watt and Green, 1982) and this, together with the increase in kazrin protein levels during keratinocyte differentiation, led us to investigate whether kazrin modulates differentiation. Kazrin overexpression stimulated differentiation whereas knockdown resulted in increased proliferation and a decreased proportion of differentiated cells. Kazrin is notable for being the only cornified envelope precursor thus far identified that regulates terminal differentiation (Candi et al., 2005).

In primary mouse keratinocytes inhibition of Rho activity has been linked to induction of terminal differentiation, whereas dominant active V14RhoA can maintain the cells in an undifferentiated state (Grossi et al., 2005). By contrast, the inhibition of terminal differentiation resulting from decreased kazrin expression was not correlated with an overall increase in active Rho, although there remains a possibility that levels of GTP-bound Rho were affected at specific cellular locations in the kazrin-knockdown cells. We did not detect a significant effect of kazrin knockdown on intercellular junction assembly during the first 2 hours after a Ca^{2+} switch; at later times (24 and 48 hours), stratification was reduced, but this could reflect the inhibition of terminal differentiation, rather than an effect on junctional dynamics (data not shown). Our current hypothesis is that kazrin regulates

desmosome assembly through inhibition of Rho, and stimulates commitment to differentiation through a Rho-independent pathway.

Recent studies in *Xenopus tropicalis* embryos demonstrate effects of kazrin that are independent of periplakin binding. Knockdown of kazrin impairs axial elongation, cell differentiation and epidermal morphogenesis in the developing embryo (Sevilla et al., 2008). A kazrin construct lacking the periplakin-binding domain can partially rescue the developmental defects associated with knockdown of kazrin. All kazrin isoforms have a nuclear localization sequence (Groot et al., 2004) and it will be interesting to investigate whether the periplakin- and Rho-independent effects of kazrin are dependent on nuclear accumulation.

Extensive studies in keratinocytes have shown that cell-substratum adhesion, mediated by integrins with involvement of Rac1, negatively regulates terminal differentiation (Benitah et al., 2005; Watt, 2001). Other more recent studies have indicated that cell-cell adhesion mediated by desmosomes and adherens junctions contributes to epidermal cell fate decisions (Elias et al., 2001; Hardman et al., 2005; Merritt et al., 2002; Tinkle et al., 2004). It is tantalizing to speculate that with its dual effects on differentiation and desmosome assembly, kazrin coordinates the onset of terminal differentiation with movement out of the epidermal basal layer.

Materials and Methods

DNA constructs and cloning

The constructs encoding N-terminally HA-tagged kazrinA, kazrinB and kazrinC in the EFplinkHA vector have been described previously (Groot et al., 2004). pCIneo kazrinA was used in all transient transfections of kazrinA with the exception of those in Fig. 2J. This construct was generated by ligating the *Xho*I fragment from EFplinkHA-kazrinA into similarly digested pCIneo. The EFplinkHA-kazrinA construct was digested with *Xho*I to release the HA-kazrinA encoding fragment, which was then blunt ended with Klenow, digested with *Sal*I and inserted into the *Sna*BI-*Sal*I sites of the pBABEpuro retroviral vector. The GFP-kazrinA fusion was created by subcloning PCR-amplified kazrinA into the *Eco*RI and *Bam*HI sites of pEGFPC2 (Clontech Laboratories, Inc.) using the following primers: forward 5′-GCG-GAATTCATGATGGAAGACAATAAG-3′, reverse 5′-GCGGGATCCCCAGTCC-GCGTCCTCCTC-3′. The N-terminally myc-tagged V14RhoA construct in EFplink2 was a gift from R. Treisman (CRUK London Research Institute, UK).

Cell culture, transfection and infection

Primary human keratinocytes from newborn foreskin (strains kv and kt, passages 2-4) were cultured and transfected as previously described (DiColandrea et al., 2000). In some cases, following a 1-2 hour recovery period after removal of the transfection mixture, the following inhibitors (Calbiochem) were added: Y27632 (15 μM), LY294002 (20 μM), AG1478 (20 μM) or 4557W (5 μM). Keratinocytes were infected with retroviral vectors as described previously (Gandarillas and Watt, 1997) and selected with 2 μg/ml puromycin (MP Biomedicals, Irvine, CA).

Antibodies

The following mouse monoclonal antibodies were used at the dilutions stated: 9E10 (1:100; anti-human myc; a gift from G. Evan, UCSF, CA), HA.11 (1:1000; anti-HA, Covance Research Products, Inc.), AC40 (1:500; anti-actin, Sigma-Aldrich), LP34 (1:100; anti-pan-keratin), clone 2-28-33 (1:5000; anti-β-tubulin, Sigma-Aldrich), 115F (1:50; anti-desmoplakin, a gift from D. R. Garrod, University of Manchester, UK), HECD-1 (1:100; anti-human E-cadherin, a gift from M. Takeichi, Riken Institute, Kobe, Japan), SY5 (1:100; anti-human involucrin), BC.1 (1:100; anti-transglutaminase 1, a gift from R. Rice, University of California, CA), Clone 55 (3 μg/ml; anti-RhoA, B and C; Millipore), Clone 26C4 (1:200; anti-RhoA; Santa Cruz Biotechnology). The rabbit antiserum Y11 (Santa Cruz Biotechnology) specific for HA was used at 1:50.

A peptide corresponding to amino acids 329-348 (DRSSTPSDINSPRHRTHSLC) of human kazrinA was used to generate antiserum LS7. LS7 was affinity purified on a column containing its immunogen coupled to Amino-Link Coupling Gel (Perbio, Erembodegem, Belgium).

For flow cytometry, SY5 and BC.1 were directly conjugated to Alexa Fluor 633 using the Protein Labeling Kit from Invitrogen. HA.11 coupled to Alexa Fluor 488 was from Covance Research Products, Inc. For immunofluorescence, Alexa Fluor 488-, 594- or 633-conjugated goat anti-rabbit or mouse IgG (Invitrogen) were diluted at 1:1000 and used for detection of primary antibodies. For immunoblotting and immunohistochemistry, HRP-conjugated donkey anti-rabbit or anti-mouse IgG was used at 1:4000 (Amersham Biosciences).

Immunofluorescence staining and confocal microscopy

Immunofluorescence staining was performed as described previously (DiColandrea et al., 2000). To visualize F-actin, TRITC- or coumarin-conjugated phalloidin (Sigma) was included in the secondary antibody incubation. DAPI (Invitrogen) was included in the secondary antibody incubation to stain nuclei. All immunolabelled samples were mounted using Mowiol (Calbiochem). Images of fluorescently labelled specimens were taken at room temperature using a LSM 510 laser scanning confocal microscope equipped with 405 nm, 488 nm, 594 nm and 633 nm lasers (Carl Zeiss, Inc.). LSM 510 software was used to acquire images using the following immersion lenses (Carl Zeiss, Inc.): 10× C-Aprochromat (numerical aperture 0.45; water correction), 25× Plan-Neofluar (numerical aperture 0.80; immersion correction), 40× C-Aprochromat (numerical aperture 1.2; water correction).

Three-dimensional reconstructions of *z*-stacks were carried out using LSM 510 software. All images were further processed using Adobe Photoshop CS2 and compiled using Adobe Illustrator CS2. For quantifications, samples were scored blindly. Metamorph 7 (Molecular Devices) was used to calculate the fluorescence pixel intensity of desmoplakin and E-cadherin at cell-cell borders. This value was determined by multiplying the average pixel intensity by the area of the defined border divided by the border length.

Automated image collection and shape factor determination

Four slides with three coverslips each of immunolabelled transfected keratinocytes were automatically examined per experiment, using the high content imaging system Discovery-1 (Molecular Devices) with a Photometrics CoolSNAP HQ camera. Fluorescent images were acquired from four fields on each coverslip using a Nikon 20′ objective (numerical aperture 0.45 lens, air correction). DAPI, FITC and TRITC fluorochromes were excited by 360 nm, 470 nm and 535 nm light, respectively. Images were interactively analyzed using Metamorph 7 (Molecular Devices) software to determine cell outlines and shape factors [$4\pi\times(\text{area}/\text{perimeter}^2)$] for individual cells.

F-actin:G-actin assay

Analysis of cellular actin was performed using the G-actin/F-actin In Vivo Assay Kit (Cytoskeleton Inc., Denver, CO) in accordance with the manufacturer's instructions.

GST pull-down assay and immunoblotting

GST pull-downs for active Rho were performed as described previously (Wells et al., 2005), using the Rho binding domain of Rhotekin fused to GST coupled to glutathione agarose (Millipore). GST pull-downs for active Rac1 were performed using the Rac1/Activation Assay Kit (Millipore). Immunoblotting was performed as described previously (Groot et al., 2004).

Time-lapse microscopy

Time-lapse recordings of cells transiently transfected with GFP-kazrinA were made with a Zeiss Axiovert 135T inverted microscope equipped with a warm box (37°C) with a CO_2 source, Hamamatsu Orca ER firewire CCD camera, xyz motorized stage, a piezo z control and a 10× PlanAPOCHROMAT objective (numerical aperture 0.32; air correction; Carl Zeiss, Inc.). Images were obtained at 5-minute intervals using AQMAdvance6 Kinetic Acquisition Manager (Medical Solutions, PLC) and subsequently prepared with Adobe ImageReady. Cell tracking was performed using Metamorph software (Molecular Devices).

Flow cytometry

Intracellular staining of keratinocytes for involucrin and transglutaminase 1 was performed as described previously (Gandarillas and Watt, 1997), except that cells were fixed in 4% paraformaldehyde for 10 minutes at room temperature and antibodies used were directly conjugated to fluorophores. Flow cytometry was performed with the BD FACSCalibur System (BD Biosciences) using BD CellQuest software. FlowJo software (Tree Star) was used to further analyze the flow cytometry data.

RNA interference

Two strategies were used to find sequences suitable for siRNA-mediated knockdown of kazrin. The first was independent design of oligonucleotides following published guidelines, which resulted in the identification of the sequence targeted by siRNA426 (AGCTGATCGGAAGCGCTTA). This sequence was cloned into the pRetroSuper (Brummelkamp et al., 2002) vector (H1 promoter). The second method was screening *Silencer*® pre-designed siRNAs (Ambion) specific for human kazrin via transfection in 293 cells using Lipofectamine 2000 (Invitrogen). This resulted in the identification of the sequence targeted by siRNA1077 (CCTGCACAACCCTATTGTA), which was cloned into pSilencer 5.1-H1 Retro (Ambion). The negative controls were the sequence for Scrambled 2 from Ambion cloned into pSilencer 5.1-H1 Retro or pRetroSuper (GTACTGCTTACGATACGG). Kazrin knockdown was assessed using quantitative RT-PCR and immunoblotting.

Silent mutations were generated in the cDNA encoding the region of kazrinA recognized by siRNA426 using the QuickChange II Site-Directed Mutagenesis Kit (Stratagene). The following primers were used to introduce four base changes, which are indicated in lowercase letters: CCTTGCAGGCCATGAAAGCcGAcCGa-AAaCGCTTAAAGGGCGAGAAGA and TCTTCTCGCCCTTTAAGCGtTTtC-GgTCgGCTTTCATGGCCTGCAAGG.

Quantitative RT-PCR

RNA from cultured keratinocytes was isolated using TriReagent (Sigma) and cDNA was generated with the Superscript First-Strand Synthesis System for RT-PCR (Invitrogen). Quantitative PCR was performed using pre-designed TaqMan gene expression assays (Applied Biosystems) with the 7900HT Fast Real-Time PCR System (Applied Biosystems). Quantification was based on ΔΔCt calculations, and all samples were compared against β2 microglobulin as an endogenous control.

Proliferation assay

Keratinocytes were seeded at a density of 2000 cells/well, in triplicate, in a 96-well plate and cultured in keratinocyte-serum-free medium for 1, 2, 5 or 7 days prior to assessment of proliferation using the MTT assay (Sigma-Aldrich) according to the manufacturer's instructions.

This work was supported by Cancer Research UK and the Wellcome Trust. L.M.S. is the recipient of a National Institutes of Health fellowship (HD42379-02). We acknowledge the support of the University of Cambridge and Hutchinson Whampoa Ltd. We are most grateful to the Light Microscopy Department in the London Research Institute for providing assistance with image acquisition and analysis. We thank Erik Sahai for helpful discussions.

References

Benitah, S. A., Frye, M., Glogauer, M. and Watt, F. M. (2005). Stem cell depletion through epidermal deletion of Rac1. *Science* **309**, 933-935.

Braga, V. M., Machesky, L. M., Hall, A. and Hotchin, N. A. (1997). The small GTPases Rho and Rac are required for the establishment of cadherin-dependent cell-cell contacts. *J. Cell Biol.* **137**, 1421-1431.

Brummelkamp, T. R., Bernards, R. and Agami, R. (2002). Stable suppression of tumorigenicity by virus-mediated RNA interference. *Cancer Cell* **2**, 243-247.

Candi, E., Schmidt, R. and Melino, G. (2005). The cornified envelope: a model of cell death in the skin. *Nat. Rev. Mol. Cell. Biol.* **6**, 328-340.

DiColandrea, T., Karashima, T., Maatta, A. and Watt, F. M. (2000). Subcellular distribution of envoplakin and periplakin: insights into their role as precursors of the epidermal cornified envelope. *J. Cell Biol.* **151**, 573-586.

Elias, P. M., Matsuyoshi, N., Wu, H., Lin, C., Wang, Z. H., Brown, B. E. and Stanley, J. R. (2001). Desmoglein isoform distribution affects stratum corneum structure and function. *J. Cell Biol.* **153**, 243-249.

Gallicano, G. I., Foshay, K., Pengetnze, Y. and Zhou, X. (2005). Dynamics and unexpected localization of the plakin binding protein, kazrin, in mouse eggs and early embryos. *Dev. Dyn.* **234**, 201-214.

Gandarillas, A. and Watt, F. M. (1997). c-Myc promotes differentiation of human epidermal stem cells. *Genes Dev.* **11**, 2869-2882.

Green, K. J., Geiger, B., Jones, J. C., Talian, J. C. and Goldman, R. D. (1987). The relationship between intermediate filaments and microfilaments before and during the formation of desmosomes and adherens-type junctions in mouse epidermal keratinocytes. *J. Cell Biol.* **104**, 1389-1402.

Groot, K. R., Sevilla, L. M., Nishi, K., DiColandrea, T. and Watt, F. M. (2004). Kazrin, a novel periplakin-interacting protein associated with desmosomes and the keratinocyte plasma membrane. *J. Cell Biol.* **166**, 653-659.

Grossi, M., Hiou-Feige, A., Tommasi Di Vignano, A., Calautti, E., Ostano, P., Lee, S., Chiorino, G. and Dotto, G. P. (2005). Negative control of keratinocyte differentiation by Rho/CRIK signaling coupled with up-regulation of KyoT1/2 (FHL1) expression. *Proc. Natl. Acad. Sci. USA* **102**, 11313-11318.

Hanakawa, Y., Amagai, M., Shirakata, Y., Yahata, Y., Tokumaru, S., Yamasaki, K., Tohyama, M., Sayama, K. and Hashimoto, K. (2002). Differential effects of desmoglein 1 and desmoglein 3 on desmosome formation. *J. Invest. Dermatol.* **119**, 1231-1236.

Hardman, M. J., Liu, K., Avilion, A. A., Merritt, A., Brennan, K., Garrod, D. R. and Byrne, C. (2005). Desmosomal cadherin misexpression alters beta-catenin stability and epidermal differentiation. *Mol. Cell. Biol.* **25**, 969-978.

Huen, A. C., Park, J. K., Godsel, L. M., Chen, X., Bannon, L. J., Amargo, E. V., Hudson, T. Y., Mongiu, A. K., Leigh, I. M., Kelsell, D. P. et al. (2002). Intermediate filament-membrane attachments function synergistically with actin-dependent contacts to regulate intercellular adhesive strength. *J. Cell Biol.* **159**, 1005-1017.

Jaffe, A. B. and Hall, A. (2005). Rho GTPases: biochemistry and biology. *Annu. Rev. Cell Dev. Biol.* **21**, 247-269.

Jefferson, J. J., Leung, C. L. and Liem, R. K. (2004). Plakins: goliaths that link cell junctions and the cytoskeleton. *Nat. Rev. Mol. Cell. Biol.* **5**, 542-553.

Jones, P. H. and Watt, F. M. (1993). Separation of human epidermal stem cells from transit amplifying cells on the basis of differences in integrin function and expression. *Cell* **73**, 713-724.

Lewis, J. E., Wahl, J. K., 3rd, Sass, K. M., Jensen, P. J., Johnson, K. R. and Wheelock, M. J. (1997). Cross-talk between adherens junctions and desmosomes depends on plakoglobin. *J. Cell Biol.* **136**, 919-934.

Magee, A. I., Lytton, N. A. and Watt, F. M. (1987). Calcium-induced changes in cytoskeleton and motility of cultured human keratinocytes. *Exp. Cell Res.* **172**, 43-53.

Merritt, A. J., Berika, M. Y., Zhai, W., Kirk, S. E., Ji, B., Hardman, M. J. and Garrod, D. R. (2002). Suprabasal desmoglein 3 expression in the epidermis of transgenic mice results in hyperproliferation and abnormal differentiation. *Mol. Cell. Biol.* **22**, 5846-5858.

Nimnual, A. S., Taylor, L. J. and Bar-Sagi, D. (2003). Redox-dependent downregulation of Rho by Rac. *Nat. Cell Biol.* **5**, 236-241.

Norvell, S. M. and Green, K. J. (1998). Contributions of extracellular and intracellular domains of full length and chimeric cadherin molecules to junction assembly in epithelial cells. *J. Cell Sci.* **111**, 1305-1318.

Riento, K. and Ridley, A. J. (2003). ROCKS: multifunctional kinases in cell behaviour. *Nat. Rev. Mol. Cell. Biol.* **4**, 446-456.

Ruhrberg, C., Hajibagheri, M. A., Parry, D. A. and Watt, F. M. (1997). Periplakin, a novel component of cornified envelopes and desmosomes that belongs to the plakin family and forms complexes with envoplakin. *J. Cell Biol.* **139**, 1835-1849.

Sevilla, L. M., Rana, A. A., Watt, F. M. and Smith, J. C. (2008). KazrinA is required for axial elongation and epidermal integrity in Xenopus tropicalis. *Dev. Dyn.* **237**, 1718-1725.

Takaishi, K., Sasaki, T., Kotani, H., Nishioka, H. and Takai, Y. (1997). Regulation of cell-cell adhesion by rac and rho small G proteins in MDCK cells. *J. Cell Biol.* **139**, 1047-1059.

Tinkle, C. L., Lechler, T., Pasolli, H. A. and Fuchs, E. (2004). Conditional targeting of E-cadherin in skin: insights into hyperproliferative and degenerative responses. *Proc. Natl. Acad. Sci. USA* **101**, 552-557.

Vasioukhin, V., Bauer, C., Yin, M. and Fuchs, E. (2000). Directed actin polymerization is the driving force for epithelial cell-cell adhesion. *Cell* **100**, 209-219.

Vasioukhin, V., Bowers, E., Bauer, C., Degenstein, L. and Fuchs, E. (2001). Desmoplakin is essential in epidermal sheet formation. *Nat. Cell Biol.* **3**, 1076-1085.

Waschke, J., Spindler, V., Bruggeman, P., Zillikens, D., Schmidt, G. and Drenckhahn, D. (2006). Inhibition of Rho A activity causes pemphigus skin blistering. *J. Cell Biol.* **175**, 721-727.

Watt, F. M. (2001). Stem cell fate and patterning in mammalian epidermis. *Curr. Opin. Genet. Dev.* **11**, 410-417.

Watt, F. M. and Green, H. (1982). Stratification and terminal differentiation of cultured epidermal cells. *Nature* **295**, 434-436.

Watt, F. M., Mattey, D. L. and Garrod, D. R. (1984). Calcium-induced reorganization of desmosomal components in cultured human keratinocytes. *J. Cell Biol.* **99**, 2211-2215.

Wells, C. M., Ahmed, T., Masters, J. R. and Jones, G. E. (2005). Rho family GTPases are activated during HGF-stimulated prostate cancer-cell scattering. *Cell Motil. Cytoskeleton* **62**, 180-194.

Wheelock, M. J. and Johnson, K. R. (2003). Cadherins as modulators of cellular phenotype. *Annu. Rev. Cell Dev. Biol.* **19**, 207-235.

Yamada, S. and Nelson, W. J. (2007). Localized zones of Rho and Rac activities drive initiation and expansion of epithelial cell-cell adhesion. *J. Cell Biol.* **178**, 517-527.

Yin, T. and Green, K. J. (2004). Regulation of desmosome assembly and adhesion. *Semin. Cell Dev. Biol.* **15**, 665-677.

Zhong, C., Kinch, M. S. and Burridge, K. (1997). Rho-stimulated contractility contributes to the fibroblastic phenotype of Ras-transformed epithelial cells. *Mol. Biol. Cell* **8**, 2329-2344.

Journal of Cell Science